# Modeling and Optimization of a Roll-Type Electrostatic Separation Process Using Artificial Neural Networks

S. Touhami , K. Medles, O. Dahou,
A. Tilmatine, S.M. IEEE, A. Bendaoud, S.M. IEEE
Electrostatics and High Voltage Research Unit IRECOM, University
Djillali Liabès Sidi Bel Abbès , Algeria
E-mail: kmedles@univ-sba.dz

L. Dascalescu, Fellow, IEEE
PPRIME Institute, UPR 3346,
CNRS - University of Poitiers - ENSMA
IUT, Angouleme 16021, France
E-mail: lucian.dascalescu@univ-poitiers.fr

***Abstract** --* The aim of this work is the development of a procedure for the optimization of electrostatic separation processes using artificial neural networks (ANN) in association with genetic algorithms. The objective was to maximize the insulation product, the control variables being the high-voltage that supplies the electrodes system and the rotation speed of the roll electrode. The ANN model is compared with that obtained using the classical experimental design methodology. The predicted optimum is confirmed by experiment.

*Index Terms*—electrostatic separator, artificial neural networks, genetic algorithms.

Fig.1: Schematic representation of the central composite faced (CCF) experimental design.

## I. INTRODUCTION

The roll-type corona-electrostatic separator [1-3] represents the most advantageous technique used in industry for the separation of conductive and nonconductive particles from granular mixtures [4]. In most applications the operation of the electrostatic separator is controlled by the high-voltage applied to the corona electrode and the speed of the grounded roll electrode. To increase the quality of separation, the adjustment of these control variables is done by examining their effects on response of the process [5-7]. Due to the complexity of the many interacting phenomena, an accurate physical model of the separator is impossible to build. This is why in previous works empirical models have been derived using experimental design methodology [8-10].

Such models enable the optimization of the process and can be employed in conjunction with fuzzy logic or genetic algorithms as tools for controlling the operation of the separators [11, 12]. It is obvious that the effectiveness of such approaches is strongly related to the accuracy of the available models and, in the case of fuzzy logic control [13], to the quality of the expert knowledge.

The aim of the present paper is to point out that the artificial neural network (ANN) techniques can accurately model the electrostatic separation, so that to facilitate the optimization of the process by the use of genetic algorithms.

## II. EXPERIMENTAL MODELLING

The experimental design methodology [14. 15] is subsequently used to derive a model that can predict the outcome of a standard roll-type corona-electrostatic separation process (i.e., the mass of the insulating product) as a function $y$ of $n$ input (control) variables $x_i$ :
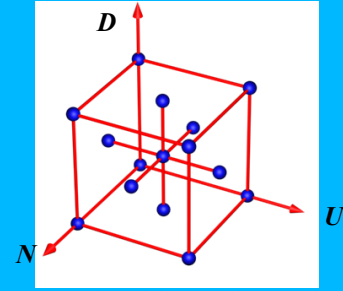
$$ y = a_0 + \sum_{i=1}^{n} a_i x_i + \sum_{i=1}^{n-1} \left( \sum_{j=i+1}^{n} a_{ij} x_i x_j \right) \tag{1} $$

where $a_i$ ($i = 1...3$) designate the coefficients of the mathematical model.

In the present work, $n = 3$ and the control variables were the following:
- Roll-speed $N$ (rev/min);
- High-voltage applied to the electrode corona $U$ (kV);
- Feed-rate $D$ (kg/h).

The experimental domain was set based on the results of previous studies carried out on a similar process [10]:

$$ 60 \text{ rev/min} \leq N \leq 100 \text{ tr/min} \tag{2} $$

$$ 26 \text{ kV} \leq U \leq 30 \text{ kV} \tag{3} $$

$$ 6 \text{ kg/h} \leq D \leq 12 \text{ kg/h} \tag{4} $$

The $a_i$ coefficients were determined from the results of a central composite faced experimental design (Fig. 1, Appendix 1). The recovery of PVC granules ($m_{PVC}$) was considered to be the response $y$ of the process of interest to this study. For each experiment $m_{PVC}$ was determined as the ratio between the mass of the PVC particles recovered in the "insulating material" compartment of the collector and the mass of PVC in the feed. The model obtained after processing the experimental data with the software MODDE 5.0 [16]:

$$ m_{PVC} \text{ [\%]} = 69.73 + 2.81n + 4.65u - 9.74d - 1.76nu + 6.78nd + 1.77ud \tag{5} $$

where $u$, $n$ and $d$ represent the normalized centered values of the control (input) variables $U$, $N$ and $D$.
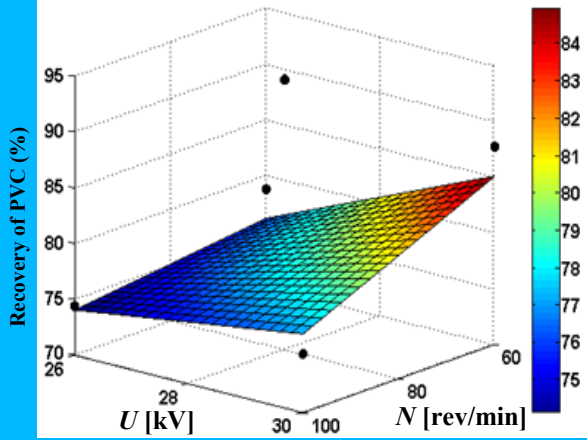
Fig.2. Model established by experimental designs (3); Dependence of PVC on $N$ and $U$ for a D = 6 kg/h; "● Experimental data"
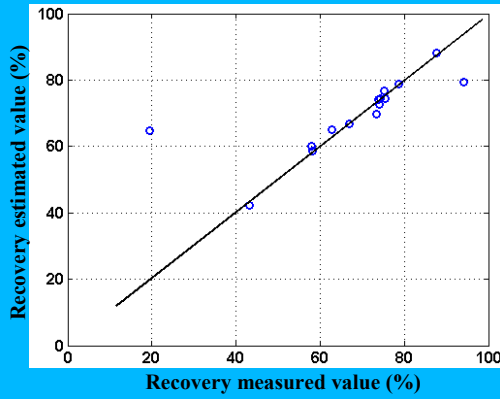


Fig.3. Prediction error of the model established by the method of the experimental design. Mean square error =153.85

Fig. 2 represents the response the process $m_{PVC} = y(N,U)$ at fixed feed-rate $D$ = 6 kg/h. The model is characterized by a high prediction error (Fig. 3), which points out the incapacity of the "linear-interaction" model (2) to reflect the outcome of the process.

### III. ARTIFICIAL NEURAL NETWORK MODELING

The artificial neural network (ANN) [17] is composed of several calculating units referred to as *neurons*. Connections between neurons in the network are characterized by numerical values called *connection weights*. A "learning" phase is necessary to determine the weights of the various connections in the network, based on the available experimental data. As a general rule, the data are divided into two sets: one will serve for *learning*, the other for the *validation* of the model. The learning set should include data over the entire operating range. The validation set is different from the previous one and is used to test the response of the network in the other experimental points. For selecting the sizes of the different data sets, a reasonable choice is to take 65% of the entire data set for training and 35% for validation.
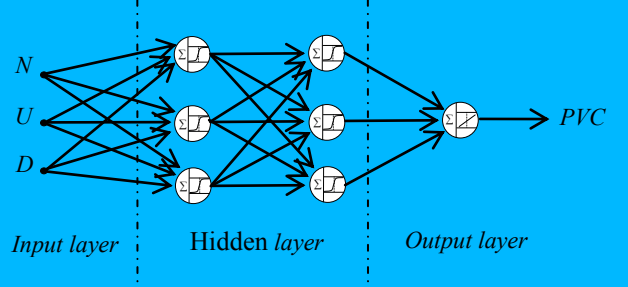


Fig.4: Feed forward artificial neural network for the modeling of the electrostatic separation process.

Currently, there exist more than 50 types ANNs used in various industry applications [17, 18]. The *feed-forward* network employed in the present study consists of four layers: an *input* layer, two *hidden* layers and an *output* layer; it receives external signals and propagates them through all the layers to obtain the "output" of the ANN. There are no feedback connections between layers. The choice of this structure is based on Kolmogorov's theorem [19. 20] that encourages the use of this type of structure in modeling of the nonlinear systems. According to this theorem, continuous functions of multiple variables can be approximated by the superposition of several continuous functions of one variable, such as the sigmoid functions [21]:

$$g(h) = \frac{1}{1 + e^{-\beta h}} \qquad (6)$$

$$g(h) = \frac{e^{\beta h} - e^{-\beta h}}{e^{\beta h} + e^{-\beta h}} \qquad (7)$$

There is no unanimously-accepted rule to establish the number of hidden layers and the number of neurons used in each layer for a given problem [18]. In spite of the fact that some researchers demonstrated the universal approximation capabilities of a feed-forward ANN with two hidden layers [20], the best structure for a given application is most often decided by applying a test and error strategy.

During the *learning* phase. the weights of connections within the network are calculated such as to minimize the difference "*e*" between the measured values of the process response and predicted values predicted by the network:

$$e = \frac{1}{N} \sum_{i=1}^{N} (\hat{y}_i - y_i)^2 \qquad (8)$$

with: $y$ - the vector of the measured values;

$\hat{y}$ - the vector of the ANN-predicted values;

$N$ – the number of experiments used for learning

Of the several algorithms specifically-developed for this operation [17], two have been tested in this study:

1- The standard *back propagation* algorithm that uses the gradient method for the optimization of the connection weights within the network [22, 23].

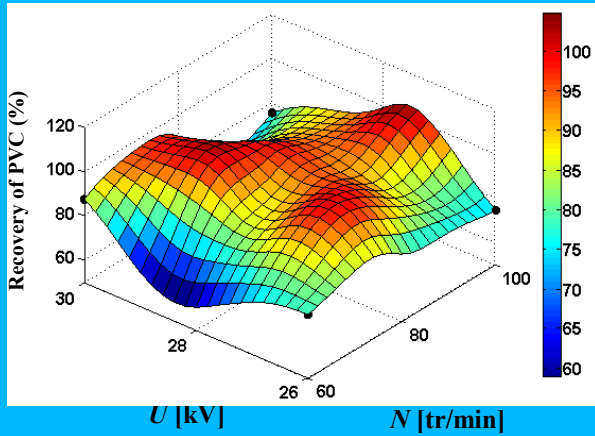2- The *Bayesian regularization process* that uses the algorithm of Levenberg-Marquardt [24].

Fig. 5. Model of PVC recovery as function of $N$ and $U$ for a $D = 6$ kg/h, established from the CCF experimental design; the weights of connections between neurons are determined by the back propagation algorithm.
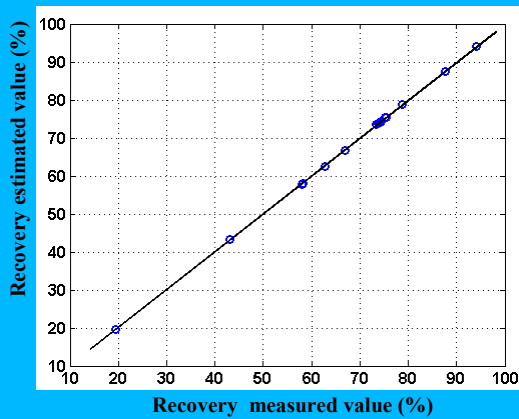


Fig. 8. Model of PVC recovery as function of $N$ and $U$ for a $D = 6$ kg/h, established from the CCF experimental design; the weights of connections between neurons are determined by the Bayesian regularization algorithm.
● Experimental data



Fig. 6. Prediction error of the model represented in Fig. 5.
Mean square error = 0.00109



Fig. 9. Prediction error of the model represented in Fig. 8.
Mean square error =1.008



Fig. 7. Generalization error of the model represented in Fig. 5.
Mean square error = 172.09
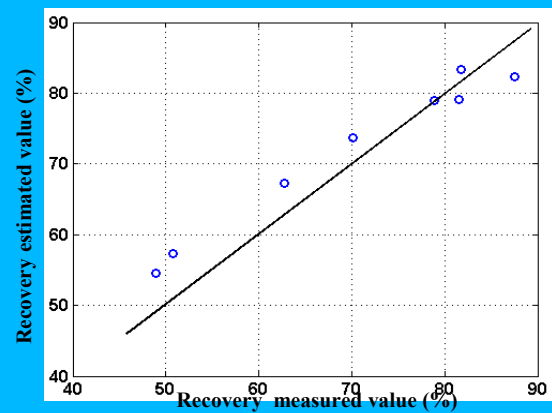


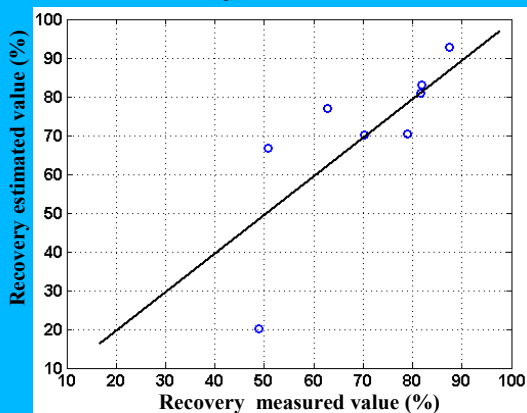Fig.10. Generalization error of the model represented in Fig. 8.
Mean square error =17.839

The application of the back propagation algorithm to an ANN having two hidden layers, each containing 6 neurons represented by sigmoid functions, has conducted to a model the response surface of which is given in Fig. 5. The model is characterized by a good predictive accuracy but an unacceptable high error of generalization [23] (Figs. 5 to 7).
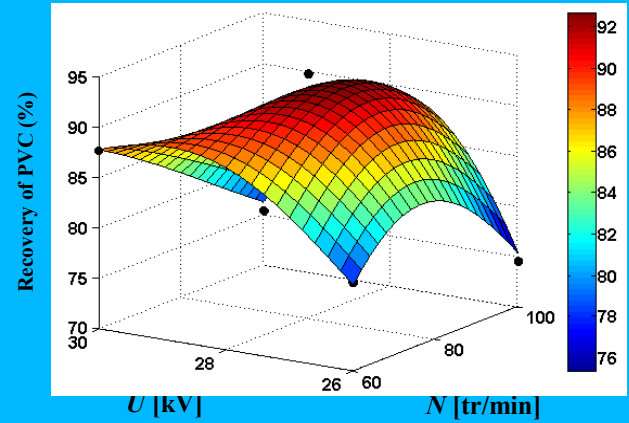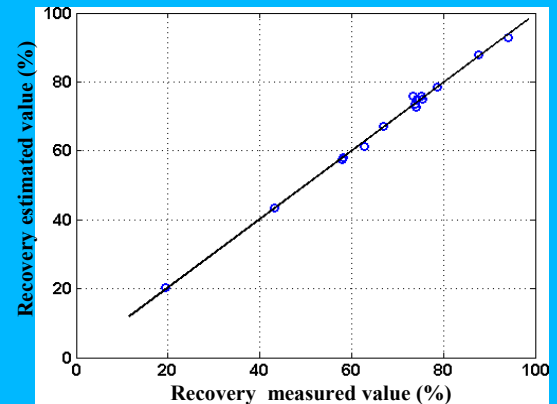
The model obtained with the Bayesian regularization process on same architecture and for the same experimental points can be examined in Fig. 8. The prediction error is lower than the measurement error 1.2% in the center of the domain (Fig. 9), but the generalization error is still unacceptably high (Fig. 10).
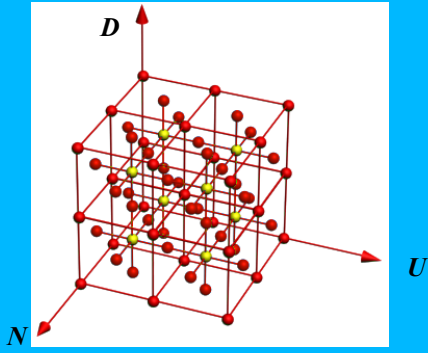
Fig. 11. Distribution of the experimental points in the domain of the study; ● learning data; ● validation data
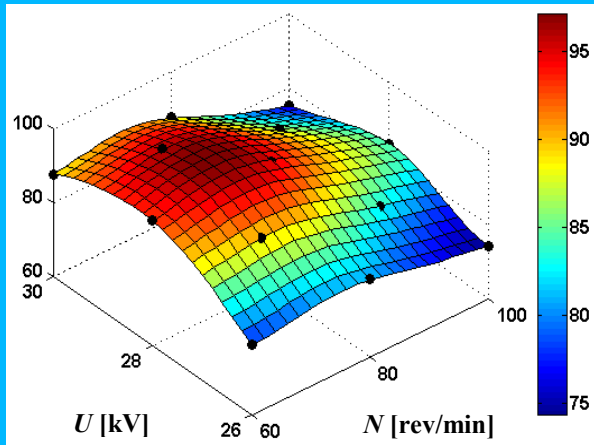


Fig. 12. Model of PVC recovery as function of $N$ and $U$ for a $D = 6$ kg/h, established from the new experimental design (71 experimental points); the weights of connections between neurons are determined by a Bayesian regularization process. ● Experimental data



Fig. 13. Prediction error of the model established by the AAN method from 71 experiments (model represented in Fig. 12).
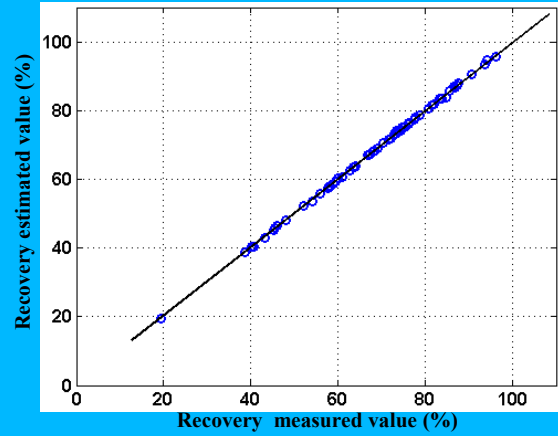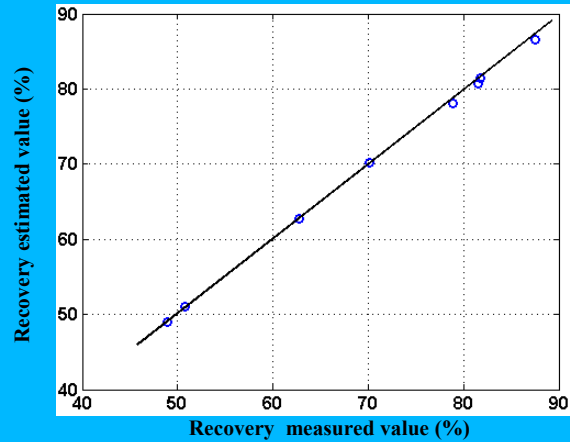Mean square error = 0.074



Fig. 14. Generalization error of the model established by the AAN method from 71 experiments (model represented in Fig. 12).
Mean square error = 0.3227

| individual | |
|---|---|
| Phenotype | |
| N [tr/min] | U [kV] |
| ↕ | ↕ |
| Gene 01 | Gene 02 |
| Genotype « Chromosome » | |
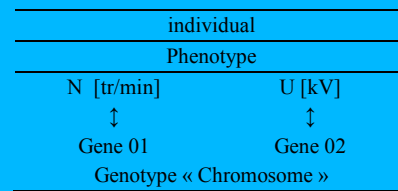
Fig. 15. Representation of the structure of an individual

To diminish the generalization error of the model, additional experiments have been carried out, in order to provide to the ANN more information on the behavior of the electrostatic separator. The distribution of the experimental points employed in the learning and validation phase is represented in the Fig. 11. By exploiting the new information, it was possible to obtain a model (Fig. 12) characterized by a mean prediction error of 0.18% and a mean generalization error of 0.43% (Figs.13 and 14).

## IV. PROCESS OPTIMIZATION

The ANN model can serve to determine the point of optimal operation of the electrostatic separator, by making use of the method of *genetic algorithms* (GA). This method employs a population of individuals (Fig. 15), represented as strings of binary characters, which undergo selection, in the presence of variation-inducing operators such as reproduction, recombination (crossover), and mutation. A fitness function is used to evaluate individuals. Reproductive success of the individuals varies with fitness. In every generation, a new set of individuals (strings) is created by using bits and pieces (chromosomes) from the fittest of the old [25].

Reproduction is a process by which individual strings are copied according to their fitness values. Copying strings according to their fitness values means that strings with higher values have a higher probability of contributing one or more offspring in the next generation. Crossover is an important operator of GA, as it produces two new individuals ("children") by recombining the chromosomes of two "parents". However, recombination does not create any new genetic material in the population. Mutation is the operator capable of overcoming this shortcoming. It involves the alteration of one individual to produce a single new solution.

To correlate the GA and the function to be optimized, the variables of the phenotype must be quantified and then binary-coded, using Gray code. The number of bits depends on the number of levels of quantification chosen by the user. For the present application, 6 bits were used for each factor, giving the possibility of quantifying the two factors in $2^6 -1 = 63$ levels, corresponding to a resolution of 0.064 kV for the voltage, and 0.0635 rev/min for the roll speed.

The structural parameters of the GA genetic algorithm were chosen as recommended in [21] and are given in Table I. To increase the performance of the algorithm the proportional selection strategy (RWS) was adopted for the selection phase, and the elitist strategy (which keeps intact the best chromosomes in moving from one generation to another) in the reproductive phase (crossover and mutation).

TABLE I. PARAMETERS OF THE GENETIC ALGORITHM

| Type of coding | Gray code |
|---|---|
| Initialization | Random |
| Type of selection | Proportional |
| Type of crossing | Two-point |
| Size of individual | 12 bits |
| Population size | 100 |
| Crossover probability | 0.95 |
| Renewal rate | 0.6 |
| Mutation probability | 0.015 |

Fig.15 shows the evolution of a population of 100 individuals for 20 generations. The optimal solution is optimal ($N$; $U$) = (72.06 rev/min; 28.35 kV). Recovery estimated in this case is $m_{PVC}$ = 97.34%. In an experiment conducted at ($N$; $U$) = (72 rev/min; 28.3 kV), the PVC recovery was $m_{PVC}$ = 97.25%, very close to the predicted value.

## V. CONCLUSIONS

The success of the control an electrostatic separation depends on the quality of the model exploited by the optimization algorithm. The use of the models of weak qualities, like the one obtained with the experimental design methodology can be misleading and generate a reduction in the performances.

The model established by ANN presented an error of prediction and generalization lower than the error of measurement. In association with GA, it enabled the determination of the optimal values of the control variables (roll speed en high-voltage), for maximizing the recovery of the insulating material contained in the feed. This model is expected to be useful for the optimal control of the electrostatic separation process.
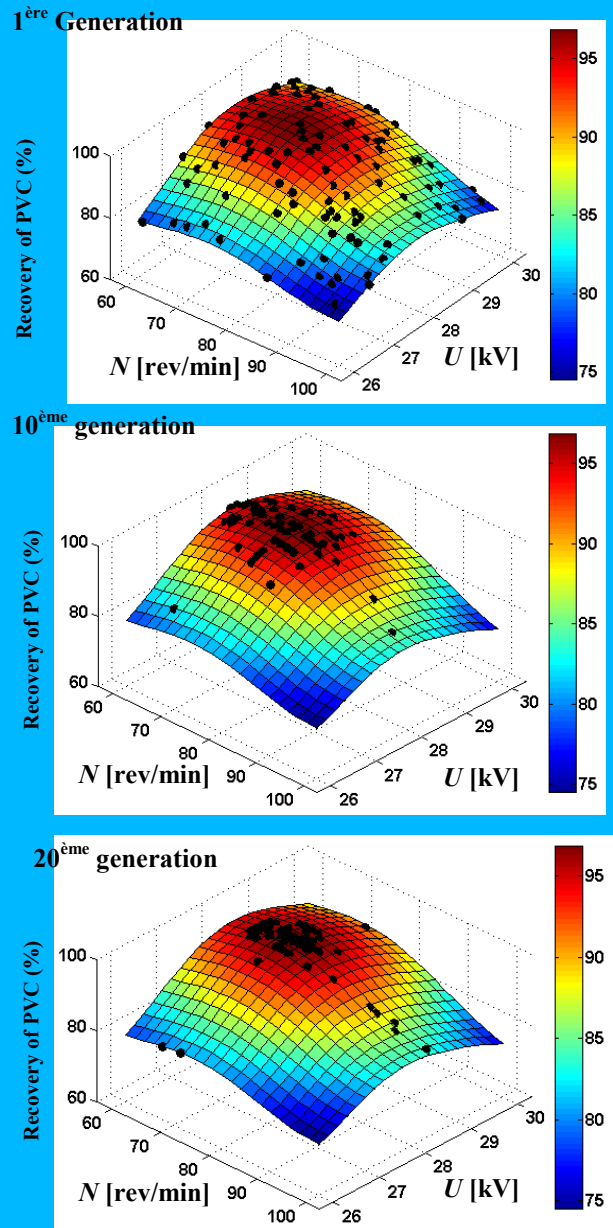


Fig. 16. Optimization of PVC recovery by genetic algorithm. The surface represents the recovery of PVC as function of $U$ and $N$ for a flow rate of 6 kg/h estimated by the model established by ANN
● individuals of the population generated by GA

REFERENCES

[1]. _____ High-tension and electrostatic separator, Eriez Magnetics, Canada, Leaflet 880-3M.SP, 1980.

[2]. _____Elektrosortierung System, Lurgi, Germany, 1518/12.84, 1984.

[3]. _____Electrostatic separation system, Mineral Deposits, Australia, Cat. No. I:SS 10923, 1989,

[4]. A. Iuga, L. Dascalescu, R. Morar, I. Csorvasy, and V. Neamtu, "Coronaelectrostatic separators for recovery of waste non-ferrous metals," J. Electrostat., vol. 23, pp. 235-243, 1989.

[5]. R. Morar, Al. Iuga, L. Dascalescu and A. Samuila, "Factors which influence the insulation-metal electro separation," J. Electrostat., vol. 30, pp. 403- 412, 1993.

[6] V. Neamtu, Al. Iuga, R. Morar, I. Suarasan, and L. Dascalescu, "Influence of high-voltage polarity on insulation-metal electro separation," *J. Electrostat.*, vol. 30, pp. 423-432, 1993.

[7] L. Dascalescu, A. Samuila, A. Iuga, R. Morar and I. Csorvasy, "Influence of material superficial moisture on insulation-metal electro separation," *IEEE Trans. Ind. Appl.*, vol. 30, pp. 844-852, 1994.

[8] M. Mihailescu, A. Samuila, A. Urs, R. Morar, A. Iuga, and L. Dascalescu, "Computer-assisted experimental design for the optimisation of electrostatic separation processes," *IEEE Trans. Ind. Appl.*, vol. 38, no. 5, pp. 1174–1181, 2002.

[9] L. Dascalescu, A. Tilmatine, F. Aman and M. Mihailescu, "Optimisation of Electrostatic Separation Processes Using Response Surface Modelling" *IEEE Trans. Ind. Appl.*, vol.40, pp. 53-59, 2004.

[10] K. Medles, A.Tilmatine, F.Miloua, A.Bendaoud, M.Younes, M.Rahli and L.Dascaluscu "Set Point Identification and Robustness Testing of Electrostatic Separation Process," *IEEE Trans. Ind. .Appl.*, vol. 43, pp. 618-626, 2007.

[11] M. Younes, A. Tilmatine, K. Medles, and L. Dascalescu "Fuzzy Control of an Electrostatic Separation Process," *IEEE Trans. Ind. Appl.*, vol. 44, pp. 09-14, 2008.

[12] O. Dahou, K. Medles, S. Touhami, M.F. Boukhoulda, A.Tilmatine, and L.Dascalescu, "Application of genetic algorithms to the optimization of a roll-type electrostatic separation process" *IEEE Trans. Ind. Appl.*, vol. 47, pp 2218-2223, 2011.

[13] I. Kiss and I. Berta, "New concept of ESP modelling based on fuzzy logic," *J. Electrostatics*, vol. 51/52, pp. 206–211, 2001.

[14] N. L. Frigon and D. Mathews, *Practical Guide to Experimental Design*. New York: Wiley, 1996.

[15] L. Eriksson, E. Johansson, N. Kettaneh-Wold, C. Wikström, and S. Wold, *Design of Experiments. Principles and Applications*. Learnways AB, Stockholm, 2000.

[16] Umetrics AB, MODDE 5.0. User Guide and Tutorial, Umetrics, Umea, Sweden, 1999

[17] V. Kecman, *Learning And Soft Computing (Support Vector Machines, Neural Networks, and Fuzzy Logic Models)*, MIT Press, 2001

[18] A.G. Looney, "Advances in feedforward neural networks: demystifying knowledge acquiring black boxes," *IEEE Trans. Knowledge & Data Eng.*, vol. 8, pp. 211–226, 1996

[19] A.N. Kolmogorov, "On the representation of continuous functions of several variables by superposition of continuous functions of one variable and addition," *Doklady Akademiia Nauk SSSR*, vol.114, pp. 953-956, 1957.

[20] V. Kurkova, "Kolmogorov's theorem and multilayer neural networks," *Neural Networks*, vol. 5, pp. 501-506, 1992.

[21] G. Cybenko, "Approximations by superposition of a sigmoidal function," *Mathematics of Control Signal and Systems*, vol. 2, pp. 202–314, 1989.

[22] M. Madan, J. Liang, and H. Noriyasu, *Static and Dynamic Neural Networks From Fundamentals to Advanced Theory*, New York: John Wiley & Sons, 2003.

[23] B. Roffel, and B. Betlem, *Process Dynamics and Control, Modeling for Control and Prediction,*New York: John Wiley & Sons, 2006

[24] M.T. Hagan, and M. Menhaj, "Training feedforward networks with the Marquardt algorithm, " *IEEE Trans. Neural Networks*, vol. 5, pp. 989-993, 1994.

[25] R.L. Haupt, and S.H. Haupt, *Practical Genetic Algorithms*. New York: Wiley-Interscience, 2004.

APPENDIX I
MASS OF THE PVC PRODUCTS OBTAINED BY CCF EXPERIMENTAL DESIGN

| N [rev/min] | U [kV] | D [kg/h] | M [g] |
|---|---|---|---|
| 60 | 26 | 6 | 78.73 |
| 100 | 26 | 6 | 74.39 |
| 60 | 30 | 6 | 87.62 |
| 100 | 30 | 6 | 75.25 |
| 60 | 26 | 12 | 43.15 |
| 100 | 26 | 12 | 19.48 |
| 60 | 30 | 12 | 58.12 |
| 100 | 30 | 12 | 73.87 |
| 60 | 28 | 9 | 66.89 |
| 100 | 28 | 9 | 74.17 |
| 80 | 26 | 9 | 62.68 |
| 80 | 30 | 9 | 75.49 |
| 80 | 28 | 6 | 94.11 |
| 80 | 28 | 12 | 57.98 |
| 80 | 28 | 9 | 73.30 |
| 60 | 26 | 6 | 78.73 |
| 100 | 26 | 6 | 74.39 |

APPENDIX II
MASS OF THE PVC PRODUCTS OBTAINED BY ADDITIONAL EXPERIMENTS
DURING THE LEARNING AND VALIDATION PHASES OF ANN MODELING

| N [rev/min] | U [kV] | D [kg/h] | M [g] |
|---|---|---|---|
| LEARNING | | | |
| 60 | 26 | 6 | 78.73 |
| 60 | 26 | 9 | 57.54 |
| 60 | 27 | 7.5 | 77.73 |
| 60 | 27 | 10.5 | 48.05 |
| 60 | 30 | 9 | 69.10 |
| 70 | 26 | 7.5 | 72.93 |
| 70 | 26 | 10.5 | 46.08 |
| 70 | 27 | 6 | 90.52 |
| 70 | 27 | 9 | 63.86 |
| 80 | 26 | 6 | 80.83 |
| 80 | 26 | 12 | 40.75 |
| 80 | 27 | 7.5 | 81.60 |
| 80 | 27 | 10.5 | 54.06 |
| 90 | 26 | 7.5 | 73.01 |
| 90 | 26 | 10.5 | 40.06 |
| 90 | 27 | 6 | 83.60 |
| 90 | 27 | 9 | 67.33 |
| 100 | 26 | 9 | 60.89 |
| 100 | 27 | 7.5 | 74.76 |
| 100 | 27 | 10.5 | 45.15 |
| 100 | 28 | 6 | 83.37 |
| VALIDATION | | | |
| 70 | 27 | 7.5 | 81.55 |
| 70 | 27 | 10.5 | 50.81 |
| 70 | 29 | 7.5 | 87.52 |
| 70 | 29 | 10.5 | 62.78 |
| 90 | 27 | 7.5 | 78.89 |
| 90 | 27 | 10.5 | 48.88 |
| 90 | 29 | 7.5 | 81.80 |
| 90 | 29 | 10.5 | 70.18 |
| 70 | 27 | 7.5 | 81.55 |
| 70 | 27 | 10.5 | 50.81 |
| 70 | 29 | 7.5 | 87.52 |